POLISH MARITIME RESEARCH 3 (127) 2025 Vol. 32; pp. 24-32
10.2478/pomr-2025-0033

VALIDATION OF CONTROL OF COURSE AND DEPTH OF BIOMIMETIC UNDERWATER VEHICLE WITH TWO SIDE AND TWO TAIL FINS

Michał Przybylski [1 *]
[1] Polish Naval Academy, Gdynia, Poland

* Corresponding author: *m.przybylski@amw.gdynia.pl*

ABSTRACT

Underwater vehicles that mimic the movements of marine animals have gained popularity in recent years due to their potential for increased manoeuvrability and efficiency. However, optimising the control systems of these vehicles for various underwater conditions remains a significant challenge due to their unconventional propulsion systems. This study is focused on the control of the course and depth of the mini CyberSeal, i.e. a biomimetic underwater vehicle equipped with two side and two tail fins. A key contribution of this research is the mathematical model of the hydrodynamic forces generated by the biomimetic propulsion system. These forces have been measured experimentally at various oscillation frequencies and fin deflections, accurately representing the propulsion dynamics for simulation and control design. Two different control strategies were implemented to achieve effective manoeuvrability: a proportional, integral, and derivative (PID) controller and a sliding mode controller (SMC). These controllers were designed to regulate the vehicle's depth and course, and their parameters were selected based on simulation results. The control strategies were verified by a comparative analysis of simulation and experimental results. The results indicate that the proposed mathematical model is sufficient to tune the controller based on the simulation, and the experimental data confirm effective depth and course control.

Keywords: biomimetic underwater vehicle, hydrodynamic model of undulating propulsion, PID, SMC control

INTRODUCTION

The exploration and increasingly frequent use of underwater space have led to significant progress and the development of autonomous underwater vehicles (AUVs), which perform a variety of missions, from scientific research to underwater surveillance and environmental monitoring [1]. Among the key problems in designing AUVs is providing efficient propulsion and control systems to perform accurate manoeuvres and ensure versatility within the underwater environment. Traditional propulsion mechanisms, i.e. propellers and jet thrusters, tend to be constrained by energy efficiency and manoeuvrability accuracy [2]. Biomimetic locomotion has been suggested as an alternative, mimicking aquatic animal motion to improve propulsion efficiency and dynamic control [3]. A significant part of the operation of such vehicles is the accurate regulation of their depth and direction; without such navigation, stability and functional effectiveness in random underwater conditions would be almost impossible. The following examines the concepts and significance of depth and heading controllers in biomimetic underwater vehicles (BUVs) and their testing [4].

This article focuses on the mini CyberSeal underwater vehicle, which uses a biomimetic propulsion system with oscillating fins inspired by the movement of aquatic creatures [5]. Unlike conventional thruster-based designs, the vehicle uses oscillating fins [6] to generate propulsion forces, increasing manoeuvrability and enabling smooth and covert observation of the underwater world. The core novelty of this research lies not merely in using: a proportional, integral, and derivative controller (PID) or sliding mode controller (SMC) strategies – which are both well-established – but in developing an experimentally derived thrust model that accurately captures the hydrodynamic forces generated by biomimetic propulsion. While previous work has relied on analytical assumptions or simulations, this study provides an empirical foundation for thrust modelling by measuring propulsion forces across various oscillation frequencies and fin angles [7]. This approach allows more realistic and adapTable simulation environments, improving the tuning and validation of control systems prior to real-world deployment.

The depth and course controllers are fundamental for the autonomous operation of underwater vehicles, enabling them to maintain desired trajectories, avoid obstacles, and perform specific tasks. Inspired by the locomotion mechanisms of aquatic creatures, biomimetic underwater vehicles present unique challenges and opportunities in control system design [8]. Various course and depth controllers are used in underwater vehicles, depending on mission requirements and the level of automation. Standard approaches, such as PID controllers [9] or model-based controllers, are generally formed by conventional strategies, i.e. adaptive algorithms [10] or SMCs. On the other hand, more advanced strategies like a linear quadratic regulator (LQR) [11], neural networks [12], or reinforcement learning [13] are used to enhance their performance and robustness.

Two different control strategies were used to adjust the depth and course of the vehicle to ensure precise manoeuvring. Because of its simplicity and effectiveness, the PID controller adjusts the control inputs based on the error between the desired and actual positions. Despite its widespread use, the PID controller can struggle with non-linearities and external disturbances commonly encountered in underwater environments. On the other hand, the SMC offers immunity to modelling inaccuracies and disturbances, making it a reliable choice in challenging and unpredicTable underwater conditions [14].

As the development of biomimetic underwater vehicles continues to evolve, the focus on verifying and optimising their control systems remains paramount. This ensures that these vehicles can operate in complex underwater environments, carrying out missions following a defined path. This increases their broader application in marine exploration, environmental monitoring, and underwater robotics. Verifying these control systems is crucial in developing the controllers and ensuring that they can handle real-world disturbances and uncertainties. Through rigorous simulations and experimental validation, researchers assess the effectiveness and reliability of these control strategies [15]. This process involves comparing different control methodologies, optimising controller parameters, and conducting extensive testing under various environmental conditions. The verification of the simulation model through experiments consisted of testing the behaviour of the mini CyberSeal during changes in course and in the depth of immersion. The verification of the course controller was carried out using the SealTracker application, a specialised tool for determining the coordinates of a moving vehicle over time [16]. An inertial measurement unit (IMU) and dedicated depth sensors were used to verify the depth controller, ensuring adequate depth change and vehicle stability accuracy. The controllers were first tested in a simulation environment and then implemented in real-world conditions to evaluate their performance. As a result, these vehicles effectively navigate and perform missions in a complex underwater world, providing greater potential for broader applications in marine biota exploration, the monitoring of aquatic environmental parameters, and further BUV development [17]. The validated control systems were then tested under real-world conditions using the mini CyberSeal. The results of this study demonstrate the utility of combining simulation-based design with real-world validation to optimise the control parameters of biomimetic underwater vehicles. Experimental validation results are presented for the PID controller, which, in the process of parameter selection, obtained the most favourable results in terms of the fitness function in both tuning and verification processes.

The paper's final part presents an analysis of the experimental results for the controller, showing that the proposed mathematical model is sufficiently accurate to develop a realistic simulation environment. The results show that the selected control parameters provide effective course and depth control, with minor differences between simulated and experimental responses, mainly due to unmodelled hydrodynamic effects – the vehicle operates at low speed in a viscous fluid [18]. The results confirm that the proposed biomimetic propulsion model and control strategies successfully translate to real-world applications.

This paper improves the mathematical model and control systems of biomimetic autonomous underwater vehicles using real-world simulation and validation. By improving the BUV's control systems, the author hopes to increase the performance and efficiency of biomimetic underwater vehicles, which may have significant uses in underwater exploration, monitoring, and surveillance [19].

MODEL OF MINI CYBERSEAL

This chapter presents the mathematical model and applied controllers of the biomimetic underwater vehicle used in the experimental verification process of the mini CyberSeal. It consists of two main subsections. The first concerns the mathematical model of a BUV with an innovative propulsion system. The second main subsection describes the controllers, optimisation methods, and fitness functions used in both the simulation and the experiment.

MATHEMATICAL MODEL

This subsection describes the design of the biomimetic underwater vehicle mini CyberSeal, particularly the new propulsion system. The following subsection presents a mathematical model of the vehicle, with special attention paid to the proposed solutions for modelling the vehicle's force and moment vector.

Fig. 1. Model of the BUV mini CyberSeal

Fig. 1 shows that the mini CyberSeal vehicle is based on the propulsion system of a seal, which has two flexible pairs of fins. The rear fins are responsible for the primary propulsion system and are used for course changes, while the side fins are used for auxiliary propulsion and dynamic draught changes. In Fig. 1, the antenna, which is used as a position marker by the SealTracker application, and the cable for the Wi-Fi antenna, which allows data transfer when the vehicle is submerged, can be seen.

In order to fine-tune the course and depth controllers of the mini CyberSeal vehicle with the new innovative undulating propulsion system, it was necessary to create a reliable mathematical model for numerical testing. The mathematical model allows simulation tests to be carried out on the vehicle to tune and test its control system. A six-degree-of-freedom motion model [20] was used to model the movement of a biomimetic submarine vehicle. The equations of motion adopted for the computer simulation take the following matrix form:

$$\mathbf{M}\dot{\mathrm{v}} = \mathbf{D}(\mathrm{v})\mathrm{v} + \mathbf{g}(\eta) = \tau \quad (1)$$

where

v – the vector of linear and angular velocities, i.e. v = [u, v, w, p, q, r];

η – the vector of vehicle position and Euler angle coordinates in the stationary system;

M – the inertia matrix (equal to the sum of the rigid body mass matrix $\mathbf{M}_{RB}$ and the associated masses matrix $\mathbf{M}_A$);

D(v) – the hydrodynamic damping matrix;

g(η) – the matrix of restoring forces (gravity forces P and buoyancy forces B);

τ – the vector of forces and moments acting on the vehicle.

From the left-hand side of Eq. (1), $\mathbf{M} \in R^{6x6}$ is the total inertia matrix, composed of the rigid body inertia matrix $\mathbf{M}_{RB}$ and the added mass matrix $\mathbf{M}_A$, $\mathbf{D}(\mathrm{v}) \in R^{6x6}$ is the hydrodynamic damping matrix, and $\mathbf{g}(\eta) \in R^{6x6}$ is the restoring vector for the BUV's hydrostatic forces. From the right-hand side of Eq. (1), $\tau \in R^{6x6}$ is the input vector of forces and moments produced by the motion of the vehicle's caudal and side fins and its orientation. For the simulation, the physical model of the BUV mini CyberSeal vehicle shown in Fig. 1 was used. The undulating propulsion system consists of two pairs of fins at the hull's rear and side. The rear fins can move at a frequency of up to 3 Hz within a range of about 80 degrees outward and up to 12 degrees relative to the vehicle's inside axis of symmetry. These fins generate the main thrust and are used for course changes. In addition, a side propulsion system is installed at the front of the vehicle hull, providing additional thrust and enabling dynamic depth changes. The side fins can also move at up to 3 Hz over a range of ±45 degrees. Both the tail and side fins are made of a combination of polycarbonate and rubber. The right side of Eq. (1) represents the vector of forces and moments of force acting on the vehicle generated by the vehicle's propulsion system:

$$\tau = [X, Y, Z, K, M, N] \quad (2)$$

where

X, Y, Z – the forces acting on the vehicle along the longitudinal, transverse, and vertical symmetry axes, respectively;

K, M, N – the moments of forces acting about the longitudinal, transverse, and vertical symmetry axes, respectively.

The thrust values generated by each fin for different frequencies and amplitudes were determined experimentally. Finally, the vehicle's speed is variable and dependent on the frequency of fin oscillations. The method of measuring the thrusts generated by the mini CyberSeal used in the mathematical equations is explained in an earlier publication [7]. More information on the mathematical dependencies of the novel drive used is contained in [19]. Table 1 shows the physical and hydrodynamic parameters used for simulating the designed BUV during experimental tasks.

Tab. 1. Mini CyberSeal physical and hydrodynamical parameters

Parameter	Symbol	Value	Units
Axial length	l	0.44	m
Fin to fin width	pw	0.22	m
Mass	m	3.245	kg
Weight	W	32.8335	N
Buoyancy	B	33.0400	N
Centre of gravity	(x_g, y_g, z_g)	(0, 0, -0.03)	m
Centre of buoyancy	(x_g, y_g, z_g)	(0, 0, 0)	m
Inertia moments	(I_{xx}, I_{yy}, I_{zz})	0.0058, 0.0506, 0.0506	$kg \cdot m^2$
Added mass terms	$X_{\dot{u}}$	0.3245	kg
	$Y_{\dot{v}}$	4.7501	kg
	$Z_{\dot{w}}$	4.7501	kg
	$K_{\dot{p}}$	0.0033	$kg \cdot m^2/rad$
	$M_{\dot{q}}$	0.0715	$kg \cdot m^2/rad$
	$N_{\dot{r}}$	0.0715	$kg \cdot m^2/rad$
Damping terms	$X_{u\|u\|}$	3.5276	$kg \cdot m$
	$Y_{v\|v\|}$	11.3461	$kg \cdot m$
	$Z_{w\|w\|}$	11.3461	$kg \cdot m$
	$K_{p\|p\|}$	0.006	$kg \cdot m^2/rad^2$
	$M_{q\|q\|}$	0.0367	$kg \cdot m^2/rad^2$
	$N_{r\|r\|}$	0.0267	$kg \cdot m^2/rad^2$

DEPTH AND COURSE CONTROLLERS

The verification of the control system is important to ensure that controllers can effectively deal with disturbances and the effects of the real environment. Researchers evaluate the effectiveness and reliability of these control strategies through rigorous simulations and experimental validations. The mini CyberSeal control system consists of two controllers. Based on the data obtained from the sensor package, each controller controls the assigned drive, affecting the vehicle's movements. The structure of the control system is shown in Fig. 2.

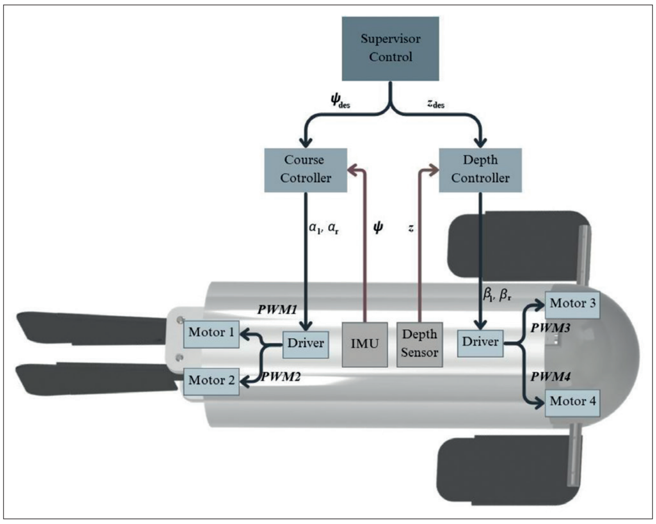

Fig. 2. Control system of the BUV mini CyberSeal

The supervisory control unit is responsible for switching specific controllers on and off at defined waypoints and calculating the desired course and depth values to keep the desired trajectory. The paper is focused on low-level control, i.e. the course and depth controllers. The mini CyberSeal vehicle course controller uses an Ocean Server OS-500 digital compass, from which the heading angle is obtained within 0.1 degrees. The control signal $u(k)$ regulates the deflection of the tail fins (α_l – left rear fin, α_r – right rear fin), which control the vehicle's course. The depth controller works by reading the actual depth of the vehicle. The vehicle is equipped with an A-10 depth sensor from the Wika company with a range of 0–11 bar and an accuracy of 0.5%. The control signal $u(k)$ from the depth controller influences the side fins (β_l – left side fin, β_r – right side fin), which makes it possible to change the vehicle depth dynamically.

The action of the PID controller is described by the following formula, presented in the discrete form:

$$u(k) = k_p e(k) + k_i \sum_{k=1}^{k_{max}} e(k) + k_d \Delta e(k), \tag{3}$$

where

1. Proportional term (P): $k_p \cdot e(k)$
   - $e(k)$ is the error at step k (difference between the setpoint and the actual value; for the course controller, it is the heading angle (Ψ) around the z_0 axis, and for the depth controller, it is the value of the z_0 position).
   - k_p is the proportional gain, determining how strongly the controller reacts to the current error.
2. Integral term (I): $k_i \cdot \sum_{k=1}^{k_{max}} e(k)$
   - $\sum_{k=1}^{k_{max}} e(k)$ is the cumulative sum of errors from the start to the current step k_{max}.
   - k_i is the integral gain, controlling how much the accumulated errors influence the controller's output. It ensures the elimination of the steady-state error.
3. Derivative term (D): $k_d \cdot \Delta e(k)$
   - $\Delta e(k)$ is the change in error between the current and previous steps (error derivative), i.e. $e(k) - e(k-1)$.
   - k_d is the derivative gain, which determines how strongly the controller reacts to the rate of error change, helping to dampen oscillations.

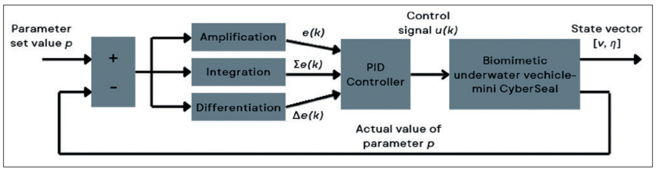

Fig. 3. Structure of PID course/depth controller of the BUV mini CyberSeal

The SMC utilised a first-order sliding surface approach with a switching control law. Its parameters (λ, k_s, φ) define the sliding surface slope, reaching law gain, and boundary layer thickness, respectively, and were tuned via the same optimisation procedure. The action of SMC is calculated using the following formulas, also presented in the discrete form:

$$s(k) = \frac{\lambda e(k) + \Delta e(k)}{\varphi}, \tag{4}$$

$$if\ |s(k)| > 1, \quad then \quad s(k) = sign(s(k)), \tag{5}$$

$$u(k) = k_s s(k), \tag{6}$$

where

1. $u(k)$ is a control signal in step k of the simulation;
2. $s(k)$ is a normalised control signal in step k of the simulation;
3. $e(k)$ is an error signal in step k of the simulation;
4. $\Delta e(k)$ is a change in the error signal in step k of the simulation, i.e. $e(k) - e(k-1)$;
5. λ, φ, ks are the constant settings of the SMC.

The influence of the control signal $u(k)$ on the deflection angles of individual fins has been limited programmatically. In the case of the rear fins, the maximum deflection angle of the outer fin is 45 degrees, while for the inner fin, it is 15 degrees relative to the axis of symmetry. The deflection angle has been limited to ±60 degrees for the side fins.

METHODOLOGY

The tuning of the course and depth controllers' parameters was performed through simulation using two controllers (PID, SMC), three optimisation methods (the Genetic Algorithm (GA), the Particle Swarm Optimization (PSO) and the Pareto Search Algorithm (PSA)), and three fitness functions [21]. Tuning and verification processes were carried out for each controller, optimisation method, and fitness function.

The tuning process was conducted for three diverse types of changes in the setpoint parameter, namely, small changes in course/depth, large changes in parameter values, and two different setpoint values. The verification process involved selecting 30 random setpoint values (for the course controller, the course change ranged from 0 to 90 degrees, and for the depth controller, from 0 to 0.7 m). For the obtained results under specific controller parameter settings, the mean value of the fitness function was calculated for all 30 verifying tests.

An earlier publication by the author [22] provides more information about the controllers' tuning process. The best fitness function results were used to determine the controllers' settings for the real object, the mini CyberSeal. The results are presented in Table 2.

Tab. 2. Parameters of mini CyberSeal [22]

PID Controller			SM Controller		
Parameter	Course	Depth	Parameter	Course	Depth
K_p	77	562	λ	**0.13**	**0.013**
K_d	2295	25194	k_s	**151.81**	**81.8**
K_i	**-0.5**	**0.01**	φ	**0.085**	**0.0035**

The experimental testing of the developed mathematical model for the mini CyberSeal biomimetic underwater vehicle was conducted in a laboratory pool of the Department of Ship Automation. The SealTracker application was used to verify the course controller by tracking the vehicle's position in the *x* and *y* planes over time [23]. Additionally, real-time data from the vehicle, including the depth, heading, pitch, and roll, were used to further verify the depth controller's performance.

RESULTS

Computer simulations were performed using the previously developed mathematical model of the mini CyberSeal. The parameters of the course and depth controllers were tuned using advanced artificial intelligent algorithms [24], and only the best results obtained during the tuning process, as shown in Table 2, based on the fitness function, were selected for the simulations and experiment. Fig. 4 compares the selected simulation results for the PID controller and SMC. These results represent the best results for each controller based on optimising the three fitness functions. The SMC, both in simulation tests and in the tuning and verification process for the different fitness functions, did not achieve better results than the PID controller. Therefore, the experimental results shown in Figs. 5 and 6 correspond only to the PID controller, which showed the best performance during the simulation-based tuning process. During the experimental tests, the vehicle was first accelerated to a constant speed of approximately 0.4 m/s at a fin oscillation frequency of 2 Hz, before the initiation of any desired course or depth change. Experimental testing was conducted in a laboratory pool, which imposed limitations on depth, course changes, and the ability to introduce disturbances.

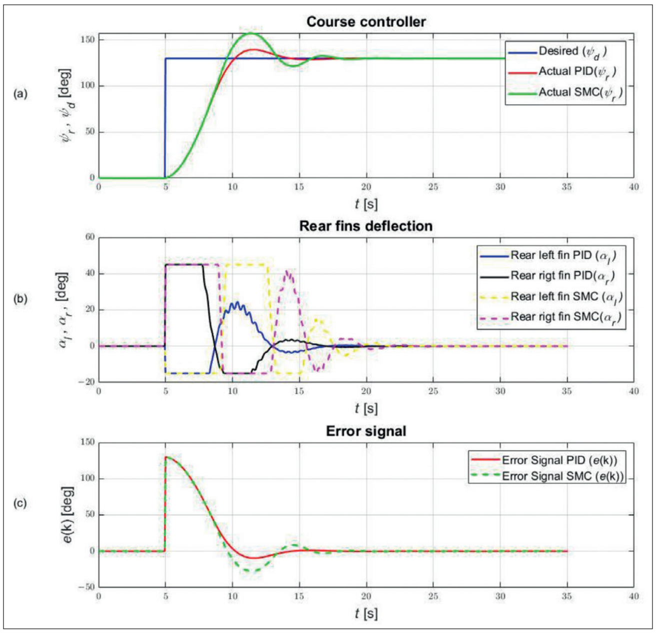

Fig. 4. Simulation model of mini CyberSeal course change for PID controller and SMC: a) change of course from an initial value of 0° to a desired value of 130°, b) deflection angles of the tail fins, c) error signal

Fig. 4 consists of three subgraphs illustrating the simulated dynamics of the mini CyberSeal underwater vehicle's course change. Each subgraph shows a different aspect of the vehicle's response to a commanded course change from 0° to 130°.

(a) Course controller response

The top graph shows the desired course ψ_d (blue line) and the response of the PID controller (red) and the SMC (green). Initially, the course is 0° and remains constant until approximately 5 s, allowing the vehicle to reach the desired speed with a fin oscillation frequency of 2 Hz. At t = 5 s, the desired course changes to 130° and the actual course begins to respond. The SMC reacts more slowly and shows a clear overshoot – it exceeds the setpoint by a noticeable amount before stabilising. The PID controller reaches the setpoint faster and more precisely. It shows no overshoot and has a shorter settling time.

(b) Rear fin deflection

The middle graph shows the left rear fin deviation (blue) and right rear fin deviation (black) for the PID controller and the SMC (yellow and magenta), respectively. For a large control signal $u(k)$, a limitation in fin deflection can be observed for 45 degrees outward and 15 degrees inward. The PID controller generates smoother and smaller swings, which may indicate better control and less control effort. On the other hand, the SMC generates more rapid, abrupt changes in yaw, especially at the beginning – this can lead to more actuator wear and less smooth operation. Once the course is established, both the PID controller and SMC aim to stabilise swings close to zero, which is the expected effect.

(c) Error signal

The bottom graph displays the error between the desired and actual course. The PID controller reduces the error faster and

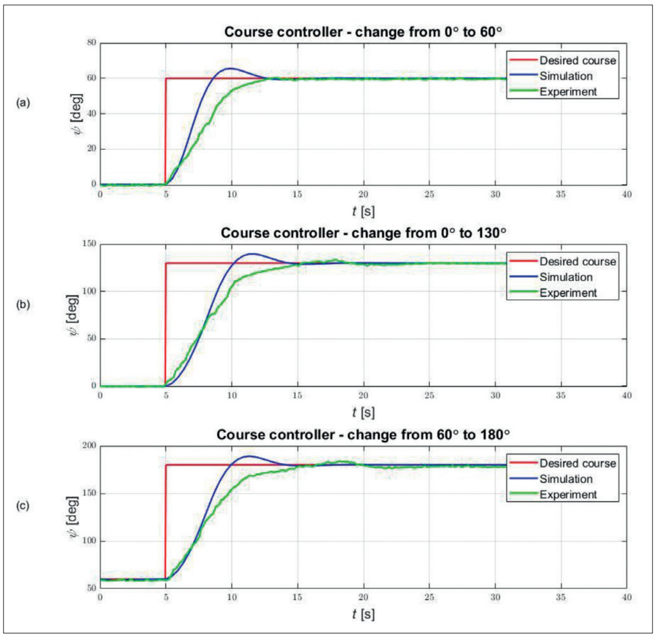

Fig. 5. Change in course of mini CyberSeal vehicle controlled by the PID controller: a) from an initial value of 0° to a desired value of 60°, b) from an initial value of 0° to a desired value of 130°, c) from an initial value of 60° to a desired value of 180°

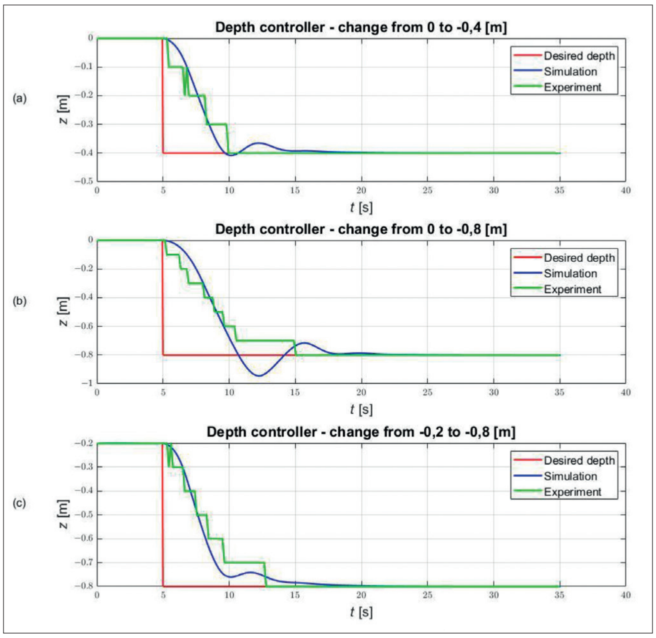

Fig. 6. Change in depth of mini CyberSeal vehicle controlled by the PID: a) from an initial value of 0 m to a desired value of 0.4 m, b) from an initial value of 0 m to a desired value of 0.8 m, c) from an initial value of 0.2 m to a desired value of 0.8 m

with less overshoot, while the SMC has a more significant visible oscillation before it stabilises, confirming that its response is less damped. At steady state (after about 15 s), both methods achieve a similar low error rate, but the PID does so faster and smoother.

Each subgraph in Fig. 5 represents a different course change scenario. The course controller (PID) effectively guides the vehicle to the desired heading in all three test cases. In each scenario, the simulation response shows a faster reaction with minor overshoot. In contrast, the experimental response is slightly slower, smoother, and more damped, indicating real-world inertia and system delays. Overall, the PID controller performs well, and the experimental results validate the simulation, with only minor differences due to real-world dynamics.

Fig. 6, on the other hand, consists of three subgraphs illustrating the depth control dynamics of the mini CyberSeal underwater vehicle. Each subgraph represents a different depth change scenario for the PID depth controller.

(a) Depth change from 0 to -0.4 m

The simulated response (blue) shows a rapid dive followed by a slight overshoot before stabilisation. The experimental response (green) follows a similar trajectory. The controller provides fast depth adjustment and works very effectively despite the depth sensor's low resolution of 0.1 m.

(b) Depth change from 0 to -0.8 m

The simulation (blue) shows a rapid descent, with some overshoot and oscillations before stabilisation. The experimental response (green) is similar but shows slightly slower dynamics and fewer oscillations. A larger change in depth results in a longer settling time. The experimental results suggest higher damping, leading to a smoother but slower transition.

(c) Depth change from -0.2 to -0.8 m

The depth is initially -0.2 m, and then it is -0.8 m at $t = 5$ s. The simulation (blue) shows a rapid descent, delay before the setpoint, and stabilisation. The experimental response (green) is similar but slightly delayed and smoother. The system behaves similarly to the previous cases, but the transition is more gradual since it starts from a non-zero initial depth. Overshoot does not occur. The experimental data suggest less aggressive controller operation, probably due to hydrodynamic effects or actuator limitations.

ANALYSIS

The evaluation of the control performance of the mini CyberSeal vehicle's course and depth contouring was carried out based on three key qualitative indicators for different course/depth change scenarios [25]:

- t_n (rising time) – the time required to reach a certain percentage of the final course/depth (90% of the setpoint);
- t_r (settling time) – the time required for the system to stabilise within a specified range around the set course/depth (±5% of the setpoint);
- M_r (magnitude of first overshoot) – the value of the first overshoot in response to the desired value.

The obtained research results allow the formulation of the following conclusions regarding the selected controller.

Table 3 presents a qualitative evaluation of the mini CyberSeal vehicle's course controller, measuring its effectiveness in controlling the heading (yaw) across different course changes. Analysing the individual qualitative indicators, the following can be concluded:

Tab. 3. Qualitative assessment of BUV course controller for real experiment (E) and simulation (S)

Controlling the heading of the mini CyberSeal underwater vehicle **Change of desired course angle from $\psi_{des1} \rightarrow \psi_{des2}$**				
Control quality indicators		0° → 60°	0° → 130°	0° → 180°
t_n [s]	E	5.25	6.45	5.85
	S	3.1	4.5	4.3
t_r [s]	E	6.5	8.25	8.95
	S	6.25	7.6	7.4
M_r [°]	E	0.3	3.2	4.3
	S	5.5	9.5	9.0

(a) Analysis of rise time (t_n)

- The rise time (t_n) is consistently higher in the experiments (E) than in the simulations (S), indicating a slower system response under real conditions.
- The highest rise time (t_n = 6.45 s in the experiment) occurs for the 0° → 130° transition, which is expected due to the larger course change.

(b) Analysis of stabilisation time (t_r)

- The experimental results (E) show smoother and more damped behaviour, with stabilisation times ranging from 6.5 to 8.95 s.
- The simulation settling times (S) for 0° → 130° and 60° → 180° are much longer (7.6 s and 7.4 s, respectively), due to the large first overshoot in the simulated model.
- The shortest tr occurs for 0° → 60°, confirming that more minor course changes stabilise faster.

(c) Overshoot analysis (M_r)

- The experimental system shows significantly less overshoot than the simulation, suggesting better natural attenuation in actual conditions.
- The largest overshoot in the experiments (M_r = 4.3°) occurs for the 60° → 180° transition, which makes sense due to the larger course correction.
- The 0° → 60° transition shows minimal overshoot, indicating that smaller course changes are more easily controlled.

To summarise the course regulator, there are differences between the experiment and simulation. The real system is slower but more sTable due to the accepted simplifications of the BUV motion model. The overshoot and settling times increase with larger course corrections, especially in simulations. The experimental results show less overshoot and more controlled transitions, which is beneficial for smooth operation. The mini CyberSeal vehicle was connected via an umbilical cord for communication and data transfer during the experiments. While the presence of the tether might have introduced a slight additional hydrodynamic damping effect, its influence on the vehicle's stabilisation is considered negligible. Therefore, the improved stabilisation observed in the experiments, compared to the simulation results, is primarily attributed to unmodelled hydrodynamic damping and fluid-structure interactions that were not captured in the numerical model.

Tab. 4. Qualitative assessment of the BUV depth controller for real experiment (E) and simulation (S)

Controlling the immersion depth of the mini CyberSeal underwater vehicle **Change of z coordinate from $Z_{des1} \rightarrow Z_{des2}$**				
Control quality indicators		0 → 0.4 [m]	0 → 0.8 [m]	2 → 0.8 [m]
t_n [s]	E	4.45	5.55	4.65
	S	4.1	5.25	4.45
t_r [s]	E	4.5	10.05	7.8
	S	8.45	11.95	8.3
M_r [°]	E	0	0	0
	S	0.035	0.15	0

Table 4 provides a qualitative assessment of the depth controller, demonstrating its successful regulation of the immersion depth of the mini CyberSeal underwater vehicle:

(a) Analysis of rise time (t_n)

- The rise time (t_n) is slightly longer for more significant depth changes. The experimental (E) and simulation (S) values are similar, with the experimental rise times being slightly longer due to the actual hydrodynamic effects – the frontal drag of the lateral fins.
- The largest rise time (t_n = 5.55 s in the experiment) is observed for the 0 → -0.8 m transition, which is expected for a deeper descent.

(b) Settlement time (t_r) analysis

- Simulation settling times (S) are similar to the experimental results (E); however, in all cases, the experiment is characterised by slightly better results.
- The settling time (t_r) is significantly longer for more extensive depth changes. The highest tr value (11.95 s in the simulation) occurs for the 0 → -0.8 m transition, which is also expected due to the greater depth adjustment.

(c) Overshoot analysis (Mr)

- The experimental results show zero overshoot (M_r = 0) in all cases, which means that the actual system does not significantly exceed the desired depth or that the overshoot value is no greater than the resolution of the depth sensor.

Smaller overshoot and shorter settling times have been observed for the real BUV compared to the simulation results. Despite measuring the draft depth in 0.1 m increments, which should have made the task more challenging for the controller, the depth controller performed very well compared to the course controller. This may be due to actuator damping or buoyancy forces that help stabilise the vehicle. Larger depth changes require more time. Both the rise time and the settling time increase for larger depth changes. The actual system exhibits greater damping, preventing overshoot, a desirable feature for underwater applications. However, the lack of overshoot may also indicate a slightly slower than optimal response.

CONCLUSION

The proposed mathematical model of the mini CyberSeal underwater vehicle has proven to be sufficient for developing a simulation model and selecting appropriate parameters for both the course and depth controllers. The analyses of the simulation and experimental results confirm that the designed controllers work effectively under real conditions, demonstrating the reliable tracking of the desired depth and course changes. The numerical and experimental research results, partially presented in Figs. 4 and 5, confirmed that artificial intelligence algorithms can successfully select the parameters of course and depth controllers for steering an underwater vehicle with predefined motion parameters. The designed control system, a significant accomplishment, can be applied to control other biomimetic underwater vehicles with different propulsion systems, as the control signals consisted of forces and moments, which were converted into fin actuation frequency and deflection via a separate algorithm specific to the given type of underwater vehicle.

The qualitative evaluation of the depth controller shows that the experimental and simulated settling times (t_n) are highly similar, with minor differences due to actual hydrodynamic effects. Settlement times (t_r) increase with larger changes in depth, as expected, but remain within accepTable limits. Notably, the absence of overshoot ($M_r = 0$) in the experimental results is a significant indicator of a well-damped and sTable response under real-world conditions, as it means that the system does not exceed the desired depth before settling.

Similarly, the performance of the course controller confirms that the real system is more sTable than the simulation model, with less overshoot and a slightly slower response. The differences in settling times between the experimental and simulated results suggest that the mathematical model could be improved to better account for hydrodynamic damping and actuator dynamics. However, despite these differences, the controller successfully guides the vehicle to the target direction with accepTable accuracy, proving that the controller parameters are correct for real-world applications.

Future work should focus on testing the system under disturbance conditions such as water currents, variable buoyancy, and external forces to further improve the model and increase the controller's resilience. This will help improve the mathematical model by incorporating unmodelled dynamics and ensure that the controller will operate reliably in more complex real-world scenarios. In addition, the potential for adaptive control strategies to be explored to improve response times for large changes in course and depth is an exciting prospect that the author looks forward to.

REFERENCES

1. González-García J, Gómez-Espinosa A, Cuan-Urquizo E, García-Valdovinos LG, Salgado-Jiménez T, Cabello JAE. Autonomous underwater vehicles: Localization, navigation, and communication for collaborative missions. Applied Sciences 2020. https://doi.org/10.3390/app10041256.
2. Carlton J. Marine propeller and propulsion. Burlington; 2007.
3. Li G, Liu G, Leng D, Fang X, Li G, Wang W. Underwater undulating propulsion biomimetic robots: A review. Biomimetics 2023. https://doi.org/10.3390/biomimetics8030318.
4. Cui Z, Li L, Wang Y, Zhong Z, Li J. Review of research and control technology of underwater bionic robots. Intell Mar Technol Syst 2023. https://doi.org/10.1007/s44295-023-00010-3.
5. Bu K, Gong X, Yu C, Xie F. Biomimetic aquatic robots based on fluid-driven actuators: A review. JMSE 2022. https://doi.org/10.3390/jmse10060735.
6. Hożyń S. An automated system for analysing swim-fins efficiency. NAŠE MORE : Znanstveni Časopis Za More i Pomorstvo 2020. https://doi.org/10.17818/NM/2020/3.9.
7. Szymak P, Przybylski M. Thrust measurement of biomimetic underwater vehicle with undulating propulsion. Maritime Technical Journal 2018. https://doi.org/10.2478/sjpna-2018-0014.
8. Morawski M, Malec M. Depth control for biomimetic and hybrid unmanned underwater vehicles. TechTrans 2021. https://doi.org/10.37705/TechTrans/e2021024.
9. Grządziela A, Hożyń S. Simulation tests of a drive shaft and propeller control subsystem for a fast boat. Polish Maritime Research 2024. https://doi.org/10.2478/pomr-2024-0018.
10. Dong Z, Li J, Liu W, Zhang H, Qi S, Zhang Z. Adptive heading control of underactuated unmanned surface vehicle based on improved backpropagation neural network. Polish Maritime Research 2023. https://doi.org/10.2478/pomr-2023-0006.
11. Wang M, Wang K, Zhao Q, Zheng X, Gao H, Yu J. LQR control and optimization for trajectory tracking of biomimetic robotic fish based on Unreal Engine. Biomimetics 2023. https://doi.org/10.3390/biomimetics8020236.
12. Śmierzchalski R, Kapczyński M. Autonomous control of the underwater remotely operated vehicle in collision situation with stationary obstacle. Polish Maritime Research 2022. https://doi.org/10.2478/pomr-2022-0043.
13. Algarín-Pinto JA, Garza-Castañón LE, Vargas-Martínez A, Minchala-Ávila LI, Payeur P. Intelligent motion control to enhance the swimming performance of a biomimetic underwater vehicle using reinforcement learning approach. IEEE Access 2025. https://doi.org/10.1109/ACCESS.2025.3544482.
14. Mat-Noh M, Mohd-Mokhtar R, Arshad MR, Zain ZM, Khan Q. Review of sliding mode control application in autonomous underwater vehicles. Indian Journal of Geo-Marine Sciences 2019. https://nopr.niscpr.res.in/handle/123456789/48867.

15. Guo X, Su S, Zuo Z. Simulation model validation of autonomous unmanned vehicle based on gray box identification and Bayesian statistics. Proceedings of the 5th International Conference on Communication and Information Processing, ACM, 2019. https://doi.org/10.1145/3369985.3370037.

16. Szymak P, Praczyk T, Pietrukaniec L, Hożyń S. Laboratory stand for research on mini CyberSeal. Measurement Automation Monitoring 2017. https://bibliotekanauki.pl/articles/114481.

17. Wang Y, Wang J, Yu L, Kong S, Yu J. Toward the intelligent, safe exploration of a biomimetic underwater robot: Modeling, planning, and control. Biomimetics 2024. https://doi.org/10.3390/biomimetics9030126.

18. Przybylski M. Mathematical model of biomimetic underwater vehicle. ECMS 2019 Proceedings, ECMS, 2019. https://doi.org/10.7148/2019-0343.

19. Aguzzi J, Costa C, Calisti M, Funari V, Stefanni S, Danovaro R, et al. Research trends and future perspectives in marine biomimicking robotics. Sensors 2021. https://doi.org/10.3390/s21113778.

20. Fossen TI. Handbook of marine craft hydrodynamics and motion control. Wiley; 2021.

21. Adeyiga JA, Sotonwa KA, Adenibuyan MT. Comparison of genetic algorithm and particle swarm optimization techniques in intelligent parking system. J Adv Mater Sci Eng 2022. https://doi.org/10.33425/2771-666X.1011.

22. Przybylski M. Selection of the depth controller for the biomimetic underwater vehicle. Electronics 2023. https://doi.org/10.3390/electronics12061469.

23. Hożyń S, Żak B. Stereo vision system for vision-based control of inspection-class ROVs. Remote Sensing 2021. https://doi.org/10.3390/rs13245075.

24. Besbes M, Zolghadri M, Costa Affonso R, Masmoudi F, Haddar M. Performance comparison of particle swarm optimization and genetic algorithm combined with A* search for solving facility layout problem. JID 2022. https://doi.org/10.3233/JID-210024.

25. Meng R, Sun A, Wu Z, Du X, Meng Y. 3D smooth path planning of AUV based on improved ant colony optimization considering heading switching pressure. Sci Rep 2023. https://doi.org/10.1038/s41598-023-39346-5.